

This species can be prepared directly by addition of solid (or a solution of) sodium borohydride to a solution of $[\text{Ni}^{\text{II}}(\text{L}_3)_2]^{2+}$ and excess triphenylphosphine in acetonitrile.

The formation of Ni(I) species in acetonitrile media was enhanced by the presence of moisture by which the solubility of sodium borohydride was promoted. However, it decreased the solubility of triphenylphosphine and also the stability of the Ni(I) species. In order to enhance both the solubility of reagents and stability of the Ni(I) species, a mixture of acetonitrile and water (9:1) was used.

The necessity of triphenylphosphine or an acetonitrile-like solvent for the isolation of a monomeric Ni(I) species and the formation of a different Ni(II) species on aerial oxidation of the Ni(I) species is consistent with the possible displacement of one of the L_3 ligands from $[\text{Ni}(\text{L}_3)_2]^{2+}$ cation with the substitution of a monodentate ligand like triphenylphosphine or acetonitrile. Formulation of such a species is consistent with the formation of a $[\text{Ni}^{\text{I}}(\text{L}_3)]^+$ species during electrochemical reduction.

The UV-visible and near-IR spectrum of the Ni(I) species obtained both in the absence and in the presence of triphenylphosphine showed similar characteristics. In the presence of triphenylphosphine, two bands at 400 ($\epsilon = 2500 \text{ mol}^{-1} \text{ cm}^{-1}$) and 370 nm ($\epsilon = 2700 \text{ mol}^{-1} \text{ cm}^{-1}$) and a broad weak band around 1380 nm ($\epsilon = 30 \text{ mol}^{-1} \text{ cm}^{-1}$) were observed. The two bands observed in the UV-visible region can be assigned to the charge-transfer transitions. Similar bands were observed in square-pyramidal Ni(I) species, as in the case of carbonyl-substituted Ni(I) cyclam.⁴⁴ The weak band observed in the near-IR region is typical of tetrahedral Ni(I) species.^{41,46} These observations do not provide any definite conclusion about the geometry of the solution species. However, they suggest that the tetrahedral

species predominantly observed at 77 K in the ESR experiments could undergo further substitution by phosphine ligands at high temperatures leading to either a trigonal-pyramidal or square-pyramidal Ni(I) species of type $[\text{Ni}^{\text{I}}(\text{NS}_2)(\text{P})_2]$. Stabilization of such five-coordinate species might be possible with smaller phosphines like trimethylphosphine. Further studies with various phosphines (of different steric hindrance or cone angle) and variable-temperature UV-visible or ESR spectroscopy will provide information on the structural aspects of these solution species. On the basis of electrochemical studies,⁴¹ proper balance of σ - and π -donors has been proposed as essential for the stabilization of Ni(I) against disproportionation to Ni(II) and Ni(0). The electrochemical and chemical behavior combined with the spectroscopic properties of the species described here provide strong evidence for the presence of a Ni(I) species in mixed coordination environment.

The data presented relate to neutral (thioether) donors. There is evidence¹⁹ that anionic sulfur centers are more feasible in decreasing the redox potential of the $\text{Ni}^{2+/3+}$ couple to values close to those found in hydrogenases. Current work underway is directed toward studies involving the open chain analogue of L_3 (detosylated form of compound 4 in Scheme I).

Acknowledgment. We thank the NSERC and University of Victoria for financial support. The assistance of K. A. Beveridge in X-ray structure determination is greatly appreciated.

Supplementary Material Available: Tables S1–S4, containing anisotropic temperature parameters, interatomic distances for hydrogen atoms, hydrogen atom bond angles, and selected interatomic distances (5 pages); Table S5, listing calculated and observed structure factors (7 pages). Ordering information is given on any current masthead page.

Contribution from the Department of Chemistry,
University of California, Berkeley, California 94720

Novel Cu_6O_{15} "Bowls" in Seven New Barium Copper Oxides: $\text{M}_6\text{Ba}_{46}\text{Cu}_{24}\text{O}_{84}$ ($\text{M} = \text{Al}, \text{Si}, \text{Ti}, \text{Fe}, \text{Ga}, \text{Ge}, \text{Zr}$)

Paul D. VerNooy, Michael A. Dixon, Frederick J. Hollander, and Angelica M. Stacy*

Received July 19, 1989

Large single crystals of a nonstoichiometric oxide with nominal formula $\text{Al}_6\text{Ba}_{46}\text{Cu}_{24}\text{O}_{84}$ (per unit cell) were grown by slow cooling of a mixture of alumina and cupric oxide in a barium hydroxide–barium chloride flux. Single-crystal X-ray methods revealed hexagonal Laue symmetry with unit cell dimensions $a = 13.1524$ (11) Å and $c = 17.3122$ (15) Å. The structure was refined in the space group $P6_3mc$ to an R value of 1.8%. This compound has a novel layered structure, and all the copper atoms are in unique bowl-shaped rings of composition Cu_6O_{15} . The crystals are shiny, black, hexagonal plates, and resistance measurements show that the compound is semiconducting. Magnetic measurements indicate that the bowls exhibit a spin $3/2$ ground state. $\text{Si}_6\text{Ba}_{46}\text{Cu}_{24}\text{O}_{84}$, $\text{Ti}_6\text{Ba}_{46}\text{Cu}_{24}\text{O}_{84}$, $\text{Fe}_6\text{Ba}_{46}\text{Cu}_{24}\text{O}_{84}$, $\text{Ga}_6\text{Ba}_{46}\text{Cu}_{24}\text{O}_{84}$, $\text{Ge}_6\text{Ba}_{46}\text{Cu}_{24}\text{O}_{84}$, and $\text{Zr}_6\text{Ba}_{46}\text{Cu}_{24}\text{O}_{84}$ were prepared by similar methods and found to be isomorphous.

Introduction

The recent discovery of superconductivity in copper oxide based materials¹ has stimulated interest in the synthesis and characterization of new cuprates. In particular, the barium–copper–oxide system is extremely interesting and has a very rich and complex chemistry. Several barium copper oxide phases have been known for some time,² but the traditional synthetic method of mixing, grinding, and firing the component oxides yields only a limited number of compounds. We have found that reacting the oxides in a flux consisting of molten barium hydroxide can lead to new barium copper oxides.^{3,4} In this paper, we present the synthesis, crystal structure, and properties of one of these new compounds, $\text{Al}_6\text{Ba}_{46}\text{Cu}_{24}\text{O}_{84}$. This formula reflects the nominal composition, given 100% occupation of all atomic sites. However, the compound

is nonstoichiometric, with many sites showing significant deviations from full occupancy.

Previous work in this laboratory has shown that molten alkali-metal and alkaline-earth-metal hydroxides are superior fluxes for the synthesis of copper oxides.^{3–5} In particular, barium hydroxide can be used to synthesize barium copper oxides by using the flux as the source of barium. Cupric oxide dissolves readily

- (1) Bednorz, J. G.; Müller, K. A. *Z. Phys. B* 1986, 64, 189.
- (2) Müller-Buschbaum, Hk. *Angew. Chem., Int. Ed. Engl.* 1977, 16, 674.
- (3) VerNooy, P. D.; Dixon, M. A.; Stacy, A. M. In *High-Temperature Superconductors*; Brodsky, M. B., Dynes, R. C., Kitazawa, K., Tuller, H. L., Eds.; MRS Symposium Proceedings, Vol. 99; Materials Research Society: Pittsburgh, PA, 1988; pp 651–654.
- (4) Dixon, M. A.; VerNooy, P. D.; Stacy, A. M. In *High Temperature Superconductors II*; Capone, D. W., Butler, W. H., Batlogg, B., Chu, C. W., Eds.; MRS Symposium Proceedings, Vol. EA14; Materials Research Society: Pittsburgh, PA, 1988; pp 69–71.
- (5) Ham, W. K.; Holland, G. F.; Stacy, A. M. *J. Am. Chem. Soc.* 1988, 110, 5214.

* To whom correspondence should be addressed.

in molten barium hydroxide (mp $\sim 450^\circ\text{C}$),⁶ and barium cuprates can be precipitated by heating the solutions to temperatures between 600 and 850 $^\circ\text{C}$. As the flux is heated, water evaporates and solid barium oxide forms; the remaining molten barium hydroxide becomes supersaturated, and crystallization of barium cuprates occurs.

The compound obtained depends on the maximum temperature, cooling rate, and the composition of the hydroxide melt. While BaCuO_2 is the only barium cuprate that we have crystallized from pure $\text{Ba}(\text{OH})_2$, sizable crystals (up to 8 mm across) of new cuprates can be obtained when chloride is added to the flux in the form of barium or cupric chloride. This basic, oxygen-rich medium has a relatively low melting point of 344 $^\circ\text{C}$ for the 92 mol % $\text{Ba}(\text{OH})_2$ -8 mol % BaCl_2 eutectic mixture;⁷ our flux is typically 13 mol % BaCl_2 .

In the presence of alumina, large, high-quality single crystals of $\text{Al}_6\text{Ba}_{46}\text{Cu}_{24}\text{O}_{84}$ can be grown from the $\text{Ba}(\text{OH})_2$ - BaCl_2 flux mixture. This compound has a novel layered crystal structure containing bowl-shaped rings made up of six copper atoms, each in square-planar coordination to four oxygen atoms. The synthesis of the compound and its crystal structure, as determined by single-crystal X-ray diffraction methods, are described below. Resistivity and magnetic measurements are also reported. $\text{Si}_6\text{Ba}_{46}\text{Cu}_{24}\text{O}_{84}$, $\text{Ti}_6\text{Ba}_{46}\text{Cu}_{24}\text{O}_{84}$, $\text{Fe}_6\text{Ba}_{46}\text{Cu}_{24}\text{O}_{84}$, $\text{Ga}_6\text{Ba}_{46}\text{Cu}_{24}\text{O}_{84}$, $\text{Ge}_6\text{Ba}_{46}\text{Cu}_{24}\text{O}_{84}$, and $\text{Zr}_6\text{Ba}_{46}\text{Cu}_{24}\text{O}_{84}$ were prepared by similar methods and found to be isomorphous. Results of physical measurements on these analogues will be published in a subsequent paper.

Experimental Section

Synthesis. A typical melt consisted of 0.33 g of neutral alumina (Super I activity, Woelm Pharma), 2.0 g of cupric oxide (ACS grade, Fisher Scientific), 2.75 g of anhydrous barium chloride (reagent grade, Fisher Scientific), and 15.0 g of anhydrous barium hydroxide (reagent grade, Fisher Scientific). All reagents were used directly from the bottle, except the barium chloride, which was dried at 100 $^\circ\text{C}$ overnight. The powders were mixed intimately, placed in a 20-mL alumina crucible, and packed down so that the crucible was about three-quarters full. A lid was placed on the crucible and secured with masking tape to ensure that it was not dislodged when put into the furnace; the masking tape burned off upon heating. Crystals were also grown by replacing the aluminum oxide with stoichiometric amounts of silicon oxide (Alfa, 99.9%), titanium dioxide (Cerac, 99.9%), ferric nitrate (Fisher, ACS grade, dried/decomposed at 100 $^\circ\text{C}$), gallium oxide (Alfa, 99.99%), germanium oxide (Cerac, 99.999%), or zirconium oxide (Johnson Matthey, 99.9975%); for these reactions, silver crucibles were used instead of an alumina crucible.

In a typical preparation, the crucible was heated from room temperature to 750 $^\circ\text{C}$ over 2.5 h, held at 750 $^\circ\text{C}$ for 5 h, and cooled to 600 $^\circ\text{C}$ over 36 h. The furnace was then shut off and allowed to cool over several hours to room temperature. The largest crystals were obtained by reducing the amount of CuO to 1 g and using a vertical tube furnace with the top of the crucible placed just below the hottest region. This kept the surface of the melt hotter than the bulk, preventing a crust from forming on top of the melt. In these cases, large plates of the cuprate formed on the surface. In other preparations, the melt was heated to 750 $^\circ\text{C}$ for 72 h and then quenched to room temperature although the crystals tended to be smaller.

The lid on the crucible was critical for this preparation, since it slowed the rate at which water was lost from the molten hydroxide. A useful side property of the flux was that it helped seal the lid to the crucible. It was observed in most cases that, during the course of the experiment, the flux "crawled" up the sides of the crucible and seeped out under the lid. Upon meeting drier air, the barium hydroxide immediately decomposed to barium oxide and cemented the lid to the crucible. With the lid cemented in place, the loss of water was slower, and larger crystals had time to form. As a negative side effect, the lid was difficult to remove once the crucible had been cooled to room temperature. The crystals typically were found exposed on the surface of the cooled flux, which made separating the crystals from the hardened flux relatively easy.

Elemental Analysis. The compositions of single crystals of $\text{Al}_6\text{Ba}_{46}\text{Cu}_{24}\text{O}_{84}$, $\text{Ga}_6\text{Ba}_{46}\text{Cu}_{24}\text{O}_{84}$, $\text{Ge}_6\text{Ba}_{46}\text{Cu}_{24}\text{O}_{84}$, and $\text{Si}_6\text{Ba}_{46}\text{Cu}_{24}\text{O}_{84}$ were determined by wavelength-dispersive X-ray fluorescence analysis, using

Table I. Crystal Parameters at 25 $^\circ\text{C}$ for $\text{Al}_6\text{Ba}_{46}\text{Cu}_{24}\text{O}_{84}$

$a = 13.1524$ (11) \AA	cryst size: $0.14 \times 0.12 \times 0.11$ mm
$b = 13.1524$ (11) \AA	$\lambda = 0.71073$ \AA
$c = 17.3122$ (15) \AA	$\rho(\text{calc}) = 5.81$ g cm^{-3}
$\alpha = \beta = 90^\circ$	$\mu(\text{calc}) = 221$ cm^{-1}
$\gamma = 120^\circ$	transm coeff = 0.83 - 1.0
$V = 2593.5$ (6) \AA^3	$g = 3.8$ (1) $\times 10^{-8}$
$Z = 1$	$R(F^2) = 1.76\%$
fw = 9070.4	$R_w(F^2) = 2.03\%$
space group: $P6_3mc$ (No. 186)	GOF = 0.762

Table II. Lattice Parameters of $\text{M}_6\text{Ba}_{46}\text{Cu}_{24}\text{O}_{84}$ Compounds

M	$a = b$, \AA	c , \AA	M	$a = b$, \AA	c , \AA
Al	13.1524 (11)	17.3122 (15)	Ti	13.2126 (12)	17.3100 (25)
Si	13.1565 (17)	17.3121 (29)	Fe	13.1964 (17)	17.3210 (34)
Ga	13.1924 (21)	17.3488 (34)	Zr	13.1592 (19)	17.3462 (12)
Ge	13.1935 (17)	17.3591 (25)			

an ARL SEMQ electron beam microprobe. For quantitative analysis, the intensities of the X-ray emissions of the single crystal were compared with those of standards. Background counts for the wavelength regions of interest were determined by measuring the background fluorescence of synthetic materials with purities in excess of 99.99%. After correction for the background and interferences, ZAF corrections⁸ were applied to the X-ray counts.

Atomic absorption spectroscopy was used to determine the compositions of $\text{Ti}_6\text{Ba}_{46}\text{Cu}_{24}\text{O}_{84}$ and $\text{Fe}_6\text{Ba}_{46}\text{Cu}_{24}\text{O}_{84}$.

X-ray Structure Determination. Precession photos of single crystals of $\text{Al}_6\text{Ba}_{46}\text{Cu}_{24}\text{O}_{84}$ showed hexagonal Laue symmetry. Further examination of the photographs revealed that the cell was primitive and that the only systematic absence was for a c -glide ($hkl, l = 2n$). Three space groups were possible: $P6_3mc$, $P6_2c$, and $P6_3/mmc$. Single-crystal intensity data were collected on an Enraf-Nonius CAD-4 diffractometer.⁹ Mo $K\alpha$ radiation ($\lambda = 0.71073$ \AA) and a monochromator of highly oriented graphite ($2\theta = 12.2^\circ$) were used. Automatic peak search and indexing procedures yielded a primitive hexagonal cell, which was used for all further work. Cell parameters refined on the setting angles of 24 reflections with 2θ greater than 33° are summarized in Table I. Precession photographs of single crystals of $\text{Si}_6\text{Ba}_{46}\text{Cu}_{24}\text{O}_{84}$, $\text{Ti}_6\text{Ba}_{46}\text{Cu}_{24}\text{O}_{84}$, $\text{Fe}_6\text{Ba}_{46}\text{Cu}_{24}\text{O}_{84}$, $\text{Ga}_6\text{Ba}_{46}\text{Cu}_{24}\text{O}_{84}$, $\text{Ge}_6\text{Ba}_{46}\text{Cu}_{24}\text{O}_{84}$, and $\text{Zr}_6\text{Ba}_{46}\text{Cu}_{24}\text{O}_{84}$ showed the same symmetry and intensity patterns as those of $\text{Al}_6\text{Ba}_{46}\text{Cu}_{24}\text{O}_{84}$. Lattice parameters for these six isotopic compounds were obtained by procedures identical with that for the aluminum compound and are summarized in Table II.

Intensities for 2915 reflections were measured ($+h, +k, +l$, $3^\circ < 2\theta < 60^\circ$) at 25 $^\circ\text{C}$ for a small piece of an as-grown crystal of $\text{Al}_6\text{Ba}_{46}\text{Cu}_{24}\text{O}_{84}$ and converted to structure factor amplitudes and their esd's by correction for scan speed, background, and Lorentz and polarization effects.¹⁰ The crystal was sealed in a capillary to prevent decomposition due to moisture. Correction for absorption was based on the azimuthal data,¹¹ which showed a variation $I_{\min}/I_{\max} = 0.82$ for the average curve. A spherical absorption correction, based on the calculated absorption coefficient, was applied in addition to the empirical absorption correction, taking the effective radius of the crystal to be 0.08 mm.¹² Examination of the hkl reflections confirmed the presence of the c -glide. Removal of these systematic absences left 2822 reflections before averaging the redundant data. Averaging yielded 1460 unique reflections. The R value of agreement¹³ based on intensity was 2.7% and on structure factors was 1.8%.

The structure was solved by Patterson methods and refined via standard least-squares and Fourier techniques. The Patterson map ruled out the possibility of a mirror plane normal to the c axis; this eliminated

(6) Plambeck, J. A. *Encyclopedia of Electrochemistry of the Elements*; Marcel Dekker, Inc.: New York, 1976; Vol. X, pp 298-300.
 (7) Seward, R. P. *J. Am. Chem. Soc.* **1945**, *67*, 1189.

(8) Armstrong, J. T. In *Microbeam Analysis—1988*; Newbury, D. E., Ed.; Proceedings of the 23rd Annual Conference of the Microbeam Analysis Society; San Francisco, CA, 1988; pp 239-246.
 (9) University of California Chemistry Department X-ray Crystallographic Facility (CHEXRAY). Enraf-Nonius software is described in: *CAD4 Operation Manual*; Enraf-Nonius: Delft, The Netherlands, Nov 1977; updated Jan 1980, et seq.
 (10) *Structure Determination Package User's Guide*; B. A. Frenz and Associates, Inc.: College Station, TX, 1985.
 (11) Reflections used for the azimuthal scans were located near $\chi = 90^\circ$, and the intensities were measured at 10° increments of rotation of the crystal about the diffraction vector.
 (12) Bond, W. L. In *International Tables for X-ray Crystallography*; Kasper, J. S., Lonsdale, K., Eds.; Kynoch Press: Birmingham, England, 1972; Vol. II, pp 302-305.
 (13) $R(I) = (\sum |I_{av}| - |I_i|) / \sum |I_i|$, where I_i are the individual measurements and I_{av} the average to which the individual measurements contribute.

Table III. Positional Parameters and Their Estimated Standard Deviations

atom	x	y	z	$B_{iso}, \text{\AA}^2$	occ ^d
Ba1	0.667	0.333	0.000	1.26 (1)	1.0
Ba2	0.000	0.000	0.21068 (7)	0.90 (1)	0.936 (3)
Ba3	0.10097 (3)	0.202	0.53514 (4)	1.04 (1)	0.895 (2)
Ba4	0.44052 (6)	0.220	0.52976 (4)	1.32 (1)	1.0
Ba5	0.28158 (6)	0.141	0.35071 (4)	0.97 (1)	1.0
Ba6	0.18879 (3)	-0.189	0.36083 (4)	1.038 (8)	0.982 (2)
Ba7	0.94495 (6)	0.472	0.37465 (4)	1.00 (1)	0.988 (2)
Ba8	0.44720 (3)	0.894	0.19380 (4)	1.41 (1)	1.0
Ba9	0.47086 (6)	0.235	0.18801 (4)	1.01 (1)	0.909 (2)
Cu1	-0.06911 (7)	0.36616 (7)	0.03145 (5)	0.78 (1)	0.974 (2)
Cu2	0.03429 (7)	0.26764 (7)	0.19248 (5)	0.81 (1)	0.962 (2)
Al1	0.333	0.667	0.3289 (4)	0.26 (9)	0.67 (1)
Al2	0.000	0.000	0.3835 (3)	0.93 (7)	0.95 (1)
Al3	0.667	0.333	0.3543 (4)	0.56 (6)	0.93 (1)
O1	0.4313 (7)	0.216	0.0265 (4)	1.3 (1)	0.98 (2)*
O2	0.0063 (5)	0.3163 (4)	-0.0367 (3)	1.14 (8)	1.0*
O3	0.4707 (4)	0.941	0.0311 (4)	1.2 (1)	0.93 (2)*
O4	0.8592 (7)	0.430	0.0963 (4)	1.1 (1)	0.96 (1)*
O5	0.2402 (7)	0.120	0.1887 (4)	1.3 (1)	1.0*
O6	-0.0217 (5)	0.3416 (5)	0.2590 (3)	1.32 (9)	1.0*
O7	0.1974 (4)	0.395	0.1959 (5)	1.6 (1)	1.0*
O8	0.1016 (4)	0.203	0.1248 (4)	1.0 (1)	1.0*
O9	0.000	0.000	0.4834 (8)	1.5 (2)	1.00 (3)*
O10	0.5185 (8)	0.259	0.3860 (5)	1.6 (1)	1.0*
O11	0.4078 (4)	0.816	0.3548 (5)	1.9 (1)	1.0*
O12	0.0733 (4)	0.147	0.3478 (5)	1.7 (1)	1.0*
O13	0.667	0.333	0.255 (1)	2.4 (4)	0.85 (4)*
O14	0.333	0.667	0.223 (3)	2.5 (9)	0.35 (4)*
O15A	0.333	0.667	0.117 (1)	1.3 (3)	0.64 (3)*
O15B	0.333	0.667	0.080 (2)	1.3 (5)	0.47 (3)*

*Starred values indicate atoms were refined with isotropic thermal parameters.

$P6_3/mmc$ as a possible space group. Refinement was carried out successfully in space group $P6_3mc$, so the third possibility was not considered. $P6_3mc$ is a chiral space group; both enantiomers were refined, and the one with the lower R value is reported here. The two most intense reflections, (006) and (330), were removed from the data set due to apparent multiple diffraction effects.

All atoms except oxygen were refined with anisotropic thermal parameters. The occupancy of each atom was also allowed to refine, as long as it remained at a total site occupancy of 100% or less. The oxygen atoms were refined with isotropic thermal parameters so as to preserve a high data-to-parameter ratio despite the refining of their occupancies.

The final residuals for 139 variables refined against the 1191 independent reflections for which $F^2 > 3\sigma(F^2)$ were $R = 1.76\%$, $R_w = 2.03\%$, and $GOF = 0.762$. The R value for all 1458 retained data was 3.28%. The quantity minimized by the least-squares routine was $\sum w(|F_o| - |F_c|)^2$, where w is the weight of a given observation. The secondary extinction parameter g was refined also,¹⁴ and its value is given in Table I. The maximum correction, gI_{max} , was 0.17. The final refinement cycle converged with a shift/error < 0.0005 , and the largest peak in the difference Fourier had an absolute value of electron density of 1.59 electrons/ \AA^3 . The p factor used to reduce the weight of the intense reflections was set to 0.03 in the final stages of refinement. The analytical forms of the scattering factors for the neutral atoms were used,¹⁵ and all scattering factors were corrected for both the real and imaginary components of the anomalous dispersion.¹⁶ A list of the values of F_o and F_c is available as supplementary material.

Magnetic Measurements. The magnetic susceptibility of as-grown $\text{Al}_6\text{Ba}_{46}\text{Cu}_{24}\text{O}_{84}$ was measured from 2.0 to 260 K in fields of 5–50 kG by using a Quantum Design SQUID magnetometer. The sample was handled in a dry atmosphere, and any remaining flux was removed from the crystals by ultrasonic cleaning in absolute methanol. The crystals were finely ground before loading into a calibrated Kel-f (poly(chlorotrifluoroethylene)) container. The magnetization of the sample was obtained by subtracting the magnetization due to the container from the measured magnetization; the magnetization of the container was 2–3 orders of magnitude smaller than the magnetization due to the sample.

(14) Zachariasen, W. H. *Acta Crystallogr.* **1963**, *16*, 1139.

(15) Cromer, D. T.; Waber, J. T. In *International Tables for X-ray Crystallography*; Ibers, J. A., Hamilton, W. C., Eds.; Kynoch Press: Birmingham, England, 1974; Vol. IV, Table 2.2B.

(16) Cromer, D. T. In *International Tables for X-ray Crystallography*; Ibers, J. A., Hamilton, W. C., Eds.; Kynoch Press: Birmingham, England, 1974; Vol. IV, Table 2.3.1.

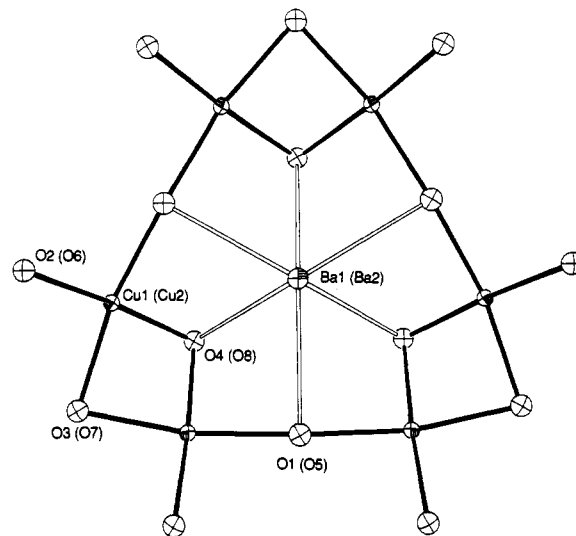


Figure 1. Perspective ORTEP diagram of Cu_2O_5 bowl and central Ba atom viewed down the 3-fold axis, showing 50% probability ellipsoids. Copper–oxygen bonds are shaded; barium–oxygen bonds are unshaded. Initial atom labels pertain to A-layer bowls; labels in parentheses pertain to B- and C-layer bowls.

The measured susceptibility was also corrected for core diamagnetism.¹⁷

Resistivity Measurements. Resistivity as a function of temperature and direction was measured on plate-shaped single crystals of $\text{Al}_6\text{Ba}_{46}\text{Cu}_{24}\text{O}_{84}$. Resistivity measurements in the plane of the plates (perpendicular to c) were made by using the four-probe van der Pauw technique.¹⁸ Through-plate (parallel to c) resistivity was measured with two probes. The crystals were kept in a dry atmosphere to prevent surface degradation. Gold contacts were sputtered onto the crystals, and in some trials, the crystals were fired at 250 °C in an O_2 atmosphere for 4 h after sputtering. Gold wires were attached to these contacts with conducting silver paint (Du Pont Conductor Composition 4929). If the paint was used directly on a crystal, the resistivity was 2 orders of magnitude greater than with the gold contacts, presumably due to decomposition of the surface. Firing the contacts lowered the resistivity even further; however, the contact resistance had little effect on the temperature dependence of the resistivity. A Keithley Model 617 electrometer and Model 220 dc current source were used for the measurements. Measurements were made between 77 and 500 K.

Results and Discussion

By use of the methods described, a large quantity of shiny, black, hexagonal plates of $\text{Al}_6\text{Ba}_{46}\text{Cu}_{24}\text{O}_{84}$ was formed. The largest of these plates had dimensions up to 8 mm across. In addition, the aluminum ions can be replaced by a +3 or +4 cation that favors tetrahedral coordination: Crystals of $\text{Si}_6\text{Ba}_{46}\text{Cu}_{24}\text{O}_{84}$, $\text{Ti}_6\text{Ba}_{46}\text{Cu}_{24}\text{O}_{84}$, $\text{Fe}_6\text{Ba}_{46}\text{Cu}_{24}\text{O}_{84}$, $\text{Ga}_6\text{Ba}_{46}\text{Cu}_{24}\text{O}_{84}$, $\text{Ge}_6\text{Ba}_{46}\text{Cu}_{24}\text{O}_{84}$, and $\text{Zr}_6\text{Ba}_{46}\text{Cu}_{24}\text{O}_{84}$ were also grown, but they were generally smaller than the aluminum compound. All the crystals are moderately moisture-sensitive; when exposed to the atmosphere, they lose their shiny appearance rapidly and will decompose in several hours.

It is interesting to note that the driving force to form $\text{Al}_6\text{Ba}_{46}\text{Cu}_{24}\text{O}_{84}$ must be strong. If copper, barium, and aluminum are present in the flux, crystals of $\text{Al}_6\text{Ba}_{46}\text{Cu}_{24}\text{O}_{84}$ usually predominate, even at temperatures and concentrations quite different from the ones given earlier. In fact, crystals of $\text{Al}_6\text{Ba}_{46}\text{Cu}_{24}\text{O}_{84}$ form even if the only source of aluminum is the alumina crucible. It also should be noted that the compound only forms in the presence of hydroxide; all attempts to synthesize $\text{Al}_6\text{Ba}_{46}\text{Cu}_{24}\text{O}_{84}$ from mixtures of the binary oxides at temperatures up to 1000 °C were unsuccessful.

Crystal Structure. $\text{Al}_6\text{Ba}_{46}\text{Cu}_{24}\text{O}_{84}$ has a layered structure. The barium and copper atoms, and most of the oxygen atoms, lie in layers perpendicular to the z axis at $z \approx 0$, $1/6$, and $1/3$ (these layers are replicated at $z \approx 1/2, 2/3$, and $5/6$ by the 6_3 screw axis). Barium

(17) O'Connor, C. J. *Prog. Inorg. Chem.* **1982**, *29*, 203.

(18) Van der Pauw, L. J. *Phillips Res. Rep.* **1958**, *13*, No. 1, 1–9.

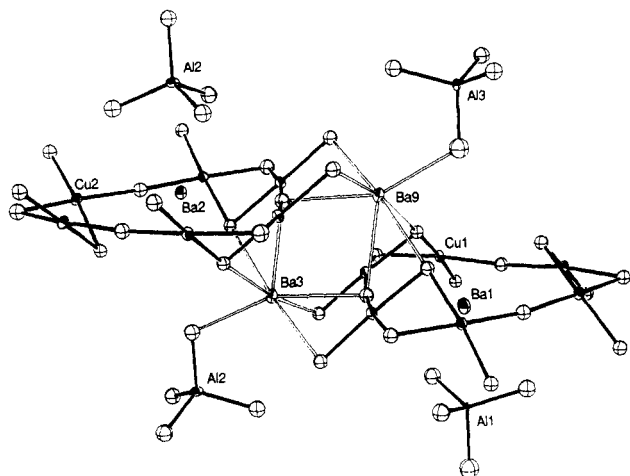


Figure 2. Perspective diagram showing closest contact of bowls in different layers, and associated AlO_4 tetrahedra. Thermal ellipsoids are at the 50% probability level.

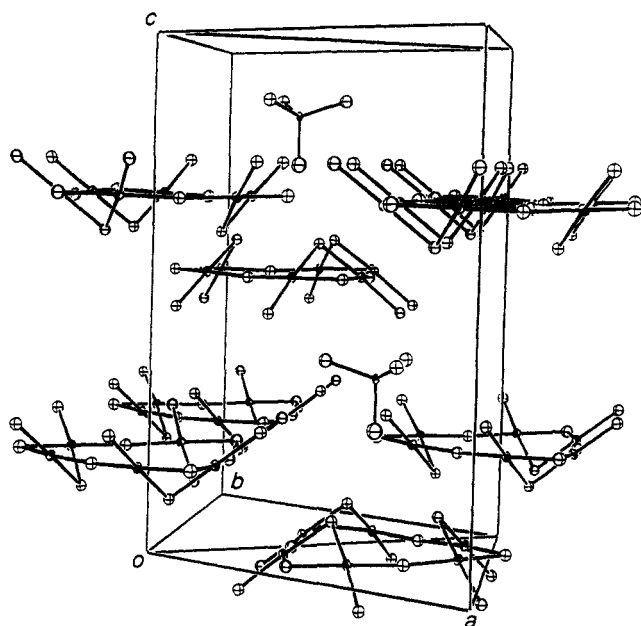


Figure 3. Unit cell diagram showing ABAC hexagonal packing of Cu_6O_{15} bowls. Also shown are the two isolated AlO_4 tetrahedra. The A-layer bowls are centered on the cell edges. The B-layer bowls are centered on one of the 3-fold axes; the C-layer bowls, on the other.

atoms are present in each of the three distinct layers, whereas the copper atoms lie only in the $z \approx 0$ and $1/6$ layers, and the aluminum atoms are found only near the $z \approx 1/3$ layer.

The unique structural feature of this compound is the isolated bowl-shaped ring of composition Cu_6O_{15} . Each copper atom in the bowl has square-planar coordination to oxygen. The CuO_4 units share oxygen atoms on one edge and one corner to form the bowl as shown in Figure 1. There are two independent bowls in the asymmetric unit, each with crystallographic C_{3v} symmetry. On the open side of this bowl is an aluminum atom coordinated by a tetrahedron of oxygen sites (Figure 2). The aluminum atom is on the 3-fold axis, and each one of the three basal oxygen atoms might be thought of as a distant fifth ligand to two copper atoms in the bowl. Occupancy refinements showed that some of the aluminum species are pyramidal AlO_3 rather than tetrahedral AlO_4 . Those aluminum atoms which are only coordinated to three oxygen atoms are missing the axial oxygen atom farthest from the bowl. There is a barium atom located on the 3-fold axis between the AlO_3 or AlO_4 moiety and the bowl.

The bowls are packed in the crystal in hexagonal layers with an ABAC/ABAC/... stacking sequence (Figure 3) and are not linked to one another by Cu–O bonds (Figure 2). The bowls in

Table IV. Selected Bond Distances and Their Estimated Standard Deviations (Å)

Ba1–Al1	2.962 (11)	Cu1–O1	1.956 (7)
Ba1–Cu1 (×6)	3.326 (1)	Cu1–O2	1.859 (8)
Ba1–O1 (×3)	2.720 (11)	Cu1–O3	1.955 (5)
Ba1–O4 (×3)	2.755 (11)	Cu1–O4	1.906 (11)
Ba1–O11 (×3)	3.032 (11)	Cu2–Cu2	2.618 (2)
Ba2–Al2	2.993 (10)	Cu2–Cu2	3.971 (2)
Ba2–Cu2 (×6)	3.332 (1)	Cu2–O5	1.988 (6)
Ba2–O5 (×3)	2.763 (12)	Cu2–O6	1.879 (9)
Ba2–O8 (×3)	2.750 (6)	Cu2–O7	1.952 (5)
Ba2–O12 (×3)	2.902 (11)	Cu2–O8	1.904 (8)
Ba4–O15A	2.990 (22)	Al1–O14	1.838 (67)
Ba4–O15B	2.721 (18)	Al1–O11 (×3)	1.755 (4)
Ba8–O14	2.642 (13)	Al2–O9	1.728 (23)
Ba8–O15A	2.911 (20)	Al2–O12 (×3)	1.780 (6)
Ba8–O15B	3.252 (34)	Al3–O13	1.722 (28)
Cu1–Cu1	2.612 (2)	Al3–O10 (×3)	1.775 (12)
Cu1–Cu1	3.907 (2)		

Table V. Selected Bond Angles and Their Estimated Standard Deviations (deg)

O1–Cu1–O2	92.6 (4)	Cu2–O5–Cu2	174.1 (7)
O1–Cu1–O4	90.9 (4)	Cu2–O7–Cu2	84.20 (8)
O2–Cu1–O3	93.9 (4)	O11–Al1–O14	104.8 (6)
O3–Cu1–O4	82.1 (3)	O11–Al1–O11	113.7 (4)
Cu1–O1–Cu1	174.3 (7)	O9–Al2–O12	110.4 (5)
Cu1–O3–Cu1	83.82 (7)	O12–Al2–O12	108.6 (5)
O5–Cu2–O6	93.0 (4)	O10–Al3–O13	108.0 (5)
O5–Cu2–O8	91.2 (4)	O10–Al3–O10	110.9 (4)
O6–Cu2–O7	94.9 (4)		
O7–Cu2–O8	81.0 (3)		

the A layer are centered on the 6_3 axis, while the bowls in the B layer are centered on one of the 3-fold axes in the unit cell. The bowls in the C layer are centered on the other 3-fold axis and are related to those in the B layer by the screw axis. The bowls in the B and C layers are inverted with respect to the bowls in the A layer. Although the A-layer bowls are crystallographically distinct from the B- and C-layer bowls, both are very similar in terms of bond distances and angles.

Distances and angles between the copper and oxygen atoms are listed in Tables IV and V. Each bowl contains six coplanar, symmetry-related copper atoms: Cu1 in the bowls in the B and C layer and Cu2 in the bowls in the A layers. O1 through O4 are bound to Cu1, and O5 through O8 are bound to Cu2. Ba1, Al1, O11, and O14 are associated with Cu1; Ba2, Al2, O9, and O12 are associated with Cu2. Within the bowl, O1 (O5) forms a single bridge between two copper atoms, while O2 (O6) is bound to only one copper atom. O3–O4 (O7–O8) form a double bridge between two copper atoms in the bowls, with O3 (O7) lying in the plane of the copper atoms and O4 (O8) out-of-plane. In both bowls, the shortest copper–oxygen distance is to the unshared oxygen atom: Cu1–O2 is 1.859 (8) Å and Cu2–O6 is 1.879 (9) Å. These short copper–oxygen bond distances indicate that the copper is highly oxidized; they are considerably shorter than the ~ 1.95 -Å bond lengths normally found in copper(II) oxides.² Both bowls also have similar occupancies for copper: 97.4 (2)% for Cu1 and 96.2 (2)% for Cu2.

The two crystallographically distinct bowls do show some differences. The O1, O3, and O4 sites in the A-layer bowls show slight deviations from full occupancy, with O3 having the lowest occupancy, at 93 (2)%. All of the oxygen sites in the B- and C-layer bowls, however, are fully occupied.

The most striking difference between the two bowls is that the aluminum atom associated with the bowls in the B and C layers (Al1) is 67 (1)% occupied and its axial oxygen atom (O14) is only 35 (4)% occupied, while the aluminum atom in the A-layer bowl (Al2) is 95 (1)% occupied and its axial oxygen (O9) is fully occupied. Thus, at least half the time, Al1 is only three-coordinate. The low occupancy of the Al1 site is probably due to the relative instability of a three-coordinate aluminum atom. Al1 is sometimes

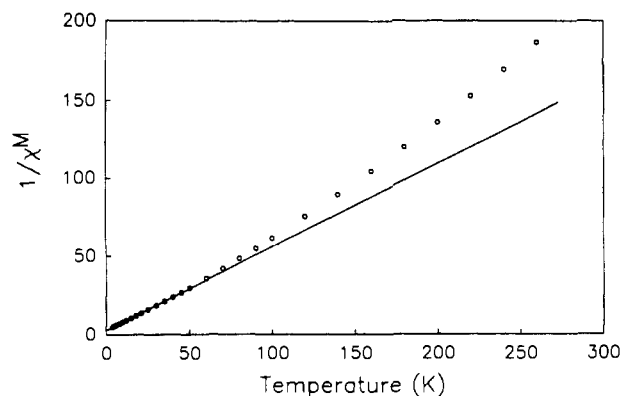


Figure 4. Inverse molar susceptibility on a per-bowl basis vs temperature for an as-grown sample of $\text{Al}_6\text{Ba}_{46}\text{Cu}_{24}\text{O}_{84}$ in a 5-kG field. A least-squares fit (shown by the line) of the linear portion at low temperature (4–50 K) yields a Curie constant per Cu_6O_{15} bowl of 1.872 (8), which is consistent with a spin $3/2$ ground state.

three-coordinate because much of the time there is apparently no room for its fourth oxygen atom. Directly below Al1 is a trigonal antiprism of barium atoms (Ba4 and Ba8). There are two oxygen sites inside the antiprism: one in the center (O15A), occupied 64 (3)% of the time, and one offset away from Al1 (O15B), occupied 47 (3)% of the time. However, O15B is sufficiently offset from the center that it does not interfere with the oxygen bonded to Al1 (O14). Within the error on their occupancies, the O15A and O15B sites need never be simultaneously occupied. If Al1 were always tetrahedrally coordinated to four oxygen atoms, its axial oxygen atom would be only 1.82 Å from O15A. This distance is considerably shorter than 2.51 Å, which is the shortest distance between fully occupied oxygen atoms in the structure, and much less than the 2.8–2.9 Å distance representative of the sum of the van der Waals radii for two oxygen atoms. Thus there is a choice between locating an oxygen atom in the center of a group of six closely spaced barium atoms and locating this oxygen far enough off-center to allow room for a single strong aluminum–oxygen bond. It is not surprising that the symmetrical coordination to all six barium atoms is slightly preferred.

Aluminum atom Al3 is found in the center of an isolated AlO_4 tetrahedron. These AlO_4 units occupy the two “octahedral holes” in the unit cell formed by the ABAC packing of the bowl-tetrahedron units (Figure 3). All of the isolated AlO_4 tetrahedra are oriented in the same direction with respect to the z axis. This orientation is the same as that of the $\text{AlO}_3/\text{AlO}_4$ moieties in the B and C layers.

The barium atoms in this structure have no favored coordination geometry. There are between seven and nine oxygen atoms coordinated to each barium atom, considering only Ba–O contacts of 3.15 Å or shorter as “coordinating”. Only three barium atoms come close to having coordination geometries that can be described simply. Ba1 and Ba2, the barium atoms that are found in the bowls just above the plane of the six copper atoms, have a distorted tricapped-trigonal-prismatic coordination. Ba7 lies in an expanded dodecahedral arrangement of oxygen atoms. All other barium atoms have coordination polyhedra best described as irregular.

The formula for the contents of one unit cell of the compound, taking into account all the partial occupancies, is $\text{Al}_{5.11(5)}\text{Ba}_{44.52(2)}\text{Cu}_{23.23(4)}\text{O}_{83.9(2)}$. This is in reasonable agreement with the results of the microprobe analysis, which yielded a composition of $\text{Al}_{4.8(3)}\text{Ba}_{42.3(9)}\text{Cu}_{24.0(8)}\text{O}_{107(5)}$. The high oxygen content given by the microprobe analysis was probably due to surface water picked up during the polishing procedure. Contamination by chloride was less than 0.08% by weight. The stoichiometries of the gallium, germanium, and silicon analogues were similarly confirmed by microprobe analysis. The stoichiometries of the titanium and iron analogues were confirmed by atomic absorption spectroscopy.

Magnetic Measurements. $\text{Al}_6\text{Ba}_{46}\text{Cu}_{24}\text{O}_{84}$ is paramagnetic to the lowest temperature measured, 2.0 K. A large dependence on field at low temperature was observed over the field range of 5–50 kG. This field dependence rules out the possibility that the copper atoms behave as isolated $S = 0$ and $S = 1/2$ ions. Instead, both the Curie constant and the saturation magnetization are consistent with each Cu_6O_{15} bowl having a spin $3/2$ ground state. A plot of inverse molar susceptibility, on a per-bowl basis, versus temperature in a 5-kG field is shown in Figure 4. Also shown is a least-squares fit to the linear portion from 4.0 to 50 K. This yields a spin-only Curie constant of 1.872 (8) and a Weiss temperature of -5.0 (3) K. An $S = 3/2$ ground state is expected to have a Curie constant of 1.875. The negative Weiss temperature is consistent with an antiferromagnetic interaction. The positive deviation of the data from the least-squares line indicates an $S = 1/2$ excited state is being populated above 50 K. A more detailed study of the magnetic properties of $\text{Al}_6\text{Ba}_{46}\text{Cu}_{24}\text{O}_{84}$ as well as the other isotopic compounds will be published in a subsequent paper.

On the basis of the formula determined from the crystal structure and with the assumption of a formal oxidation state of -2 for oxygen, $+2$ for barium, and $+3$ for aluminum, the average oxidation state for the copper atoms is $+2.73$ (2). This compares favorably with the magnetic measurement for the as-grown crystals, which would require an average oxidation state for copper of $+2.5$ (three “Cu(II)s” and three “Cu(III)s” per bowl).

Resistivity Measurements. For the entire temperature range measured (77–500 K), the resistivity varied inversely with temperature, indicating that the material is a semiconductor. The absolute resistivity is also consistent with semiconducting behavior. The lowest values measured at room temperature were 1.5 (2) $\times 10^2 \Omega \text{ cm}$ perpendicular to c and 1.4 (3) $\times 10^3 \Omega \text{ cm}$ parallel to c ; higher values were probably due to contact resistance. The large resistivities and semiconducting behavior result from the lack of a conduction pathway either parallel or perpendicular to c . The Cu_6O_{15} bowls are isolated from one another, never coming closer than about 3.5 Å (Figures 2 and 3).

Summary

Single crystals of seven new copper oxides, $\text{Al}_6\text{Ba}_{46}\text{Cu}_{24}\text{O}_{84}$, $\text{Si}_6\text{Ba}_{46}\text{Cu}_{24}\text{O}_{84}$, $\text{Ti}_6\text{Ba}_{46}\text{Cu}_{24}\text{O}_{84}$, $\text{Fe}_6\text{Ba}_{46}\text{Cu}_{24}\text{O}_{84}$, $\text{Ga}_6\text{Ba}_{46}\text{Cu}_{24}\text{O}_{84}$, $\text{Ge}_6\text{Ba}_{46}\text{Cu}_{24}\text{O}_{84}$, and $\text{Zr}_6\text{Ba}_{46}\text{Cu}_{24}\text{O}_{84}$, have been precipitated from a barium hydroxide–barium chloride flux mixture. The crystal structure of $\text{Al}_6\text{Ba}_{46}\text{Cu}_{24}\text{O}_{84}$ has been determined, and its magnetic and electronic properties were measured. This compound contains a unique bowl-shaped feature consisting of six copper atoms, each coordinated to four oxygen atoms in a square-planar array. Because the short copper–oxygen bonds are confined to these isolated bowls, the compound is semiconducting and shows localized magnetic moments. The stoichiometry, short copper–oxygen bond distances, and measured magnetic moment all indicate that this material is highly oxidized, with a formal oxidation state above Cu(II). In contrast, cuprates prepared by high-temperature reactions of intimate mixtures of metal oxides generally yield compounds with formal oxidation states of Cu(II) or lower. This suggests that new structure types are possible with the use of hydroxide fluxes as solvents. Indeed, we have isolated five new ternary and quaternary cuprates in the past year, the structures of which will be published shortly.

Acknowledgment. This work was supported by a Presidential Young Investigator Award from the National Science Foundation (Grant CHE83-51881) to A.M.S. and matching funds from E. I. du Pont de Nemours and Co. We wish to thank Dr. Barry Snyder for helpful discussions and John Donovan for assistance with the microprobe analysis. P.D.V. also thanks the NSF for a graduate student fellowship. A.M.S. thanks the Sloan Foundation and the Dreyfus Foundation for their support.

Supplementary Material Available: Tables of anisotropic thermal parameters, interatomic distances less than 3.5 Å, and bond angles (5 pages); a listing of calculated and observed structure factors (9 pages). Ordering information is given on any current masthead page.